Wear 320 (2014) 34–40

Contents lists available at ScienceDirect

Wear

journal homepage: www.elsevier.com/locate/wear

Friction, wear and plastic deformation of Cu and α/β brass under lubrication conditions

Alexey Moshkovich, Vladyslav Perfilyev, Igor Lapsker, Lev Rapoport *

Holon Institute of Technology, Holon 5810201, Israel

ARTICLE INFO

Article history:
Received 29 June 2014
Received in revised form
26 August 2014
Accepted 31 August 2014
Available online 6 September 2014

Keywords:
Friction and wear
Plastic deformation
Cooper and brass
Stacking fault energy

ABSTRACT

Friction, wear and plastic deformation of copper (Cu) and α/β brass were studied under lubrication conditions. Hardness and microstructure of surface layers were evaluated. The friction properties were presented by Stribeck curves. The friction coefficient and wear of brass were significantly larger in comparison to Cu. The critical load of transition from the elasto-hydrodynamic lubrication (EHL) to boundary lubrication (BL) was two times lower for brass. Superplastic deformation of α-phase grains in brass is appeared under friction in BL, whereas plastic deformation localized at thin surface layers is observed for Cu. Intragranular sliding in α-phase is accompanied with the formation of shear bands and many pores coalesced to cracks. Thickness of the wear particles of brass is close to the width of shear bands. The deformation hardness of brass is significantly higher in comparison to Cu rubbed in the BL region.

1. Introduction

Copper (Cu) and its alloys are widely used as engineering materials for various rubbed machine parts. Friction and wear properties of Cu and Cu alloys are determined mainly by plastic deformation and fracture in surface layers e.g. [1–3]. At the same time, these parameters depend on the stacking fault energy (SFE). Friction behavior of Cu–Al alloys in vacuum was studied by Buckley [4]. The author concludes: the lower the SFE with increasing the concentration of Al, the higher is the friction coefficient. Blau [5] studied the effect of the SFE on the wear rate for Cu–3.2Al and Cu–7.5Al in dry friction and showed that the wear rate is increased with decreasing the SFE. The similar results were obtained for aluminum bronze [6]. Sadykov with colleagues analyzed the structure and wear properties of Cu, α/β brass and CuAlFe bronze [7]. The results indicate an essential effect of some structural parameters (grain size, phase composition, texture) on wear resistance of these materials. The dry sliding friction and wear behavior of nanocrystalline Cu–Zn layers fabricated by powder compacting process were studied in Ref. [8]. The tribo-surface film covering entire worn surface effectively improved the tribological properties of nanocrystalline surface layer annealed at 300 °C. This tribo-surface film was found to comprise elements from both the sliding counterparts. Friction and wear properties of CuZn39Pb3 alloy under atmospheric and vacuum conditions have been recently studied [9]. The authors consider the adhesive wear as the dominant mechanism in the dry friction of this alloy. It is noted that increasing pressure leads to severe plastic deformation with the formation of a fine grain structure in surface layers. The lubrication function of Pb is appeared due to high flash temperature obtained in surface layers. Thus, it is seen that the friction and wear properties of Cu alloys are mainly determined by grain size, phase composition, texture and SFE parameters.

Recently, it was found that the deformation hardening of nanocrystalline surface layers of Cu under friction in the boundary lubrication (BL) regime is close to the behavior of refined structure of Cu obtained by different methods of severe plastic deformation (SPD) [10]. Steady state friction in the elasto-hydrodynamic lubrication (EHL) and BL regimes was considered as a result of the dynamic recovery based on thermally activated processes of accumulation and annihilations of dislocations. Grain refinement is achieved through the accumulation of dislocations and subsequent rearrangement by dynamic recovery or recrystallization during SPD of face-centered cubic (F.C.C.) metals and alloys e.g. [11–16]. For these materials, the small grain size and saturated crystalline defects introduced during the SPD enhance frequently a propensity for necking/plastic instability in the subsequent deformation. Shear banding is a crucial event of the microstructural behavior of F.C.C. metals at large plastic deformation. In particularly, the plastic deformation of CuZn alloys was widely studied. From the large number of studies is known that CuZn alloy (α/β brass) can exhibit a superplastic ductility in tension at testing temperatures of 800–900 K [17–19]. For instance, 60–40% CuZn alloy showed 550% elongation at 600 °C and 8.33×10^{-4} s^{-1} strain

* Corresponding author. Tel./fax: +972 3502 6616.
E-mail address: rapoport@hit.ac.il (L. Rapoport).

http://dx.doi.org/10.1016/j.wear.2014.08.016
0043-1648/

rate [19]. At this case, little slip in the α-phase, and intragranular slip in the β-phase are observed. Superplastic deformation is accompanied with cavitation due to formation and coalescence of voids [17–19]. Using Equal Channel Angular Pressing (ECAP) as a method of SPD, a superplastic elongation of 640% was recently achieved for 60–40% CuZn alloy in tension and at a temperature of 673 K [20]. It is 200° lower in comparison to the previous works. In relation to friction, the similar temperatures can be obtained in contact spots. It is known that the flash temperature in the interface of rubbed surfaces can achieve 750–800 °C [21]. For instance, Wang et al. [22] demonstrated the temperature rise to hundreds of degree Celsius close to the surface. At this case, it is expected that SPD of α/β brass due to friction and relatively high flash temperature can also lead to superplastic deformation of surface layers.

Based on the analysis of the published results it can be concluded that a majority of the friction and wear experiments with Cu alloys have been performed in dry friction conditions when the adhesion, ploughing and abrasion are the dominant mechanisms of wear. The analysis of friction and wear as well as plastic deformation and strain hardening of Cu alloys in lubrication conditions, are practically absent. Therefore, the object of this work was: to compare the friction and wear properties of Cu and α/β brass rubbed in the lubrication conditions, to evaluate the hardness and plastic deformation of surface layers. It is expected that the structure and work hardening of brass in lubrication conditions varies similar to that observed under SPD of Cu alloys.

2. Experimental procedure

For friction pin-on-disk tests, the disks (diameter, $d=40$ mm) made from the steel (AISI 1040) and hardened up to HRc=40, slide against the flat pin (diameter, $d=8$ mm) of pure (99.98 wt%) Cu, or commercial brass alloy. Flat surface of the pin was used in order to provide the constant contact pressure during long-time friction tests with different loads. Brass as an example of two-phase engineering material has been chosen. In order to provide plastic deformation mainly in a soft counterbody, the hardened steel disk-soft Cu/brass pin pairs were used. The composition of brass alloy is depicted in Table 1. In order to obtain the same virgin grain size ($d=30$–40 μm), the Cu samples were annealed at 400 °C during 1 h and the brass samples were annealed at 300 °C during 2 h. The grain structure of Cu and brass samples is shown in Fig. 1. The relationship between α- and β-phases in virgin state is 70:30.

The composition and hardness of α-and β-phases are shown in Table 2.

The sliding velocity was constant, $v=0.35$ m/s as in our previous experiments. To identify the different lubrication regimes, the Stribeck curves were used. The effect of load (P) on the friction coefficient and wear rate of Cu and brass was studied. The load was varied between 150 and 3200 N (contact pressure (p) was within, 3–64 MPa). The friction force, displacement (wear loss) and temperature near the contact were measured. Six drops of the synthetic oil, PAO-4, with viscosity of 18 mPa s at 40 °C were supplied to the contact range each minute. Careful running-in process was performed during 5 h with the virgin load not more than 150 N ($p\sim3$ MPa). In order to study the friction and damage development in different lubrication regions, the load was increased in steps of 20 N (0.4 MPa) each 20 min. The tests in the steady friction state (the EHL or BL regions) were continued during 2–3 h. Three pairs were studied at each load. The bearing ratio and probability distribution as well as, the parameters of roughness (R_a and R_z) before and after friction were measured. The virgin roughness of disks and pins, (R_a), was about 0.1 μm. The hardness tests have been used extensively for characterization of the surface layers before and after friction. In order to measure the hardness of thin surface layers, a load of 0.05 N was applied (a depth of the indenter penetration was about ~1 μm). Thirty measurements were performed for decreasing the spread of the results in the analysis of the microhardness in thin layers. The surfaces of Cu and brass samples before and after friction have been studied using SEM technique. Cu galvanic coatings were used in order to protect the friction surfaces on damage during preparation. After that, the samples were carefully cut perpendicular and parallel to the direction of friction. The arrows in all SEM images indicate the sliding direction in friction.

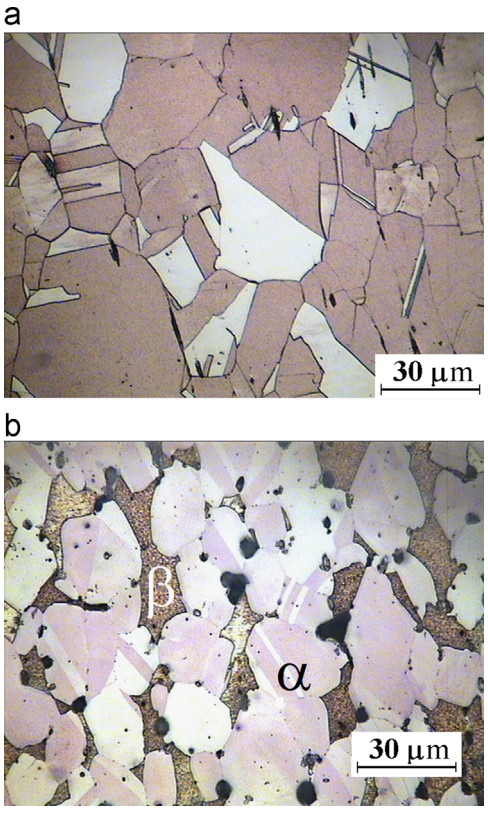

Fig. 1. Microstructure of copper (a) and brass (b) samples at virgin state. Black spots on the surface of brass are the Pb inclusions.

Table 2
The composition of Zn and the hardness of α and β phases.

	Zn (wt%)	Microhardness (MPa)
α-Phase	38 ± 0.5	1500 ± 50
β-Phase	44 ± 0.5	1900 ± 50

Table 1
Chemical composition of brass, wt%.

Cu	Pb	Zn	Al	As	Cd	Fe	Mn	Ni	Sn	As+Sb	Other
58.5	2.86	37.97	0.005	0.01	0.01	0.256	0.01	0.093	0.235	0.027	0.024

3. Results

The Stribeck curves for Cu and brass are shown in Fig. 2. It can be seen that the friction coefficient in the EHL region is low (μ=0.01–0.02). The transition to the BL region for Cu occurs at much higher load in comparison to brass (P=2450 ± 750 N and 850 ± 200 N, respectively). Maximal value of the friction coefficient in the BL region for Cu was about 0.1, while it was close to 0.2 for brass. The temperature of contact was increased with a load, Fig. 3. Maximal temperatures in the BL region are 100 °C and 120 °C for brass and Cu, respectively. Higher temperature for Cu was obtained under much higher load, 1050 N and 3200 N for brass and Cu, respectively. Furthermore, the statistic analysis of the surfaces after friction was performed. The Abbott–Firestone bearing ratio and the probability distribution graphs for Cu and brass rubbed in the BL region are shown in Fig. 4. The maximal depth of damage under friction of brass is two times larger than for Cu samples, 10 μm and 5 μm, respectively, Fig. 4a.

The probability distribution demonstrates the maximal number of grooves with a depth of 2 μm and 6 μm for Cu and brass, respectively, Fig. 4b. The roughness parameters, R_a and R_z were also measured after friction, Fig. 5. A definite correlation was observed between the friction coefficient and the roughness parameters. With increasing the friction coefficient the roughness parameters also increased. The values of roughness parameters for brass samples were significantly higher than for Cu samples, especially in the BL region. Wear of brass in the BL region was significantly higher than for Cu (2.65×10^{-4} mm^3/N m and 9.5×10^{-7} mm^3/N m, respectively). It is important to note that

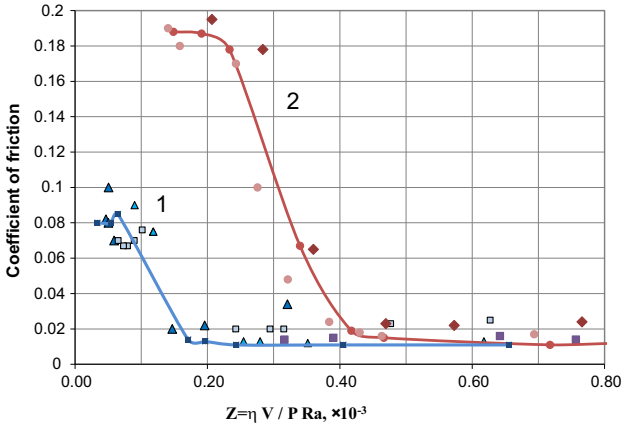

Fig. 2. Stribeck curves for copper–steel (1) and brass–steel (2) pairs. Different signs indicate the repeated tests. The X-axes is the Sommerfeld number.

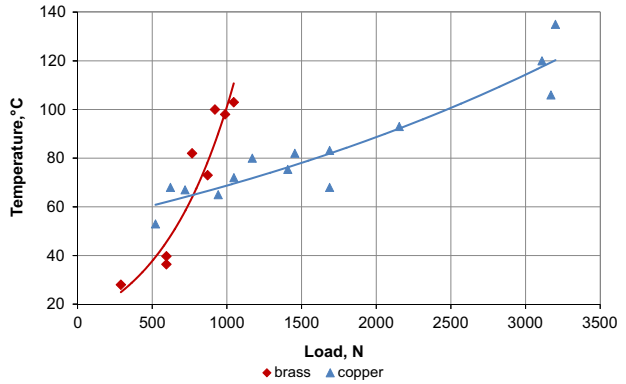

Fig. 3. The effect of load on the temperature of surface layers for brass–steel and Cu–steel pairs rubbed in different lubrication conditions.

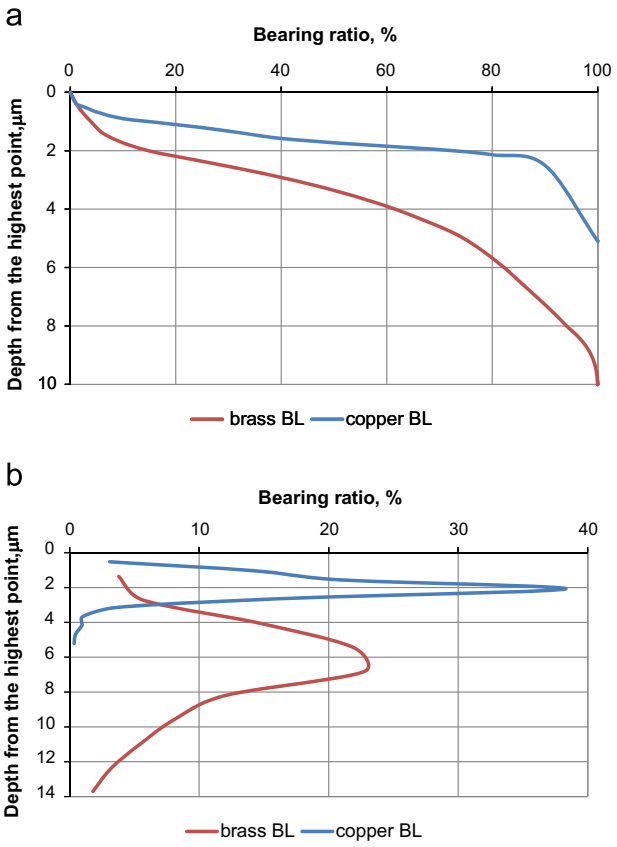

Fig. 4. The Abbott–Firestone bearing ratio (a) and the probability distribution (b) graphs for Cu and brass after friction in the BL region.

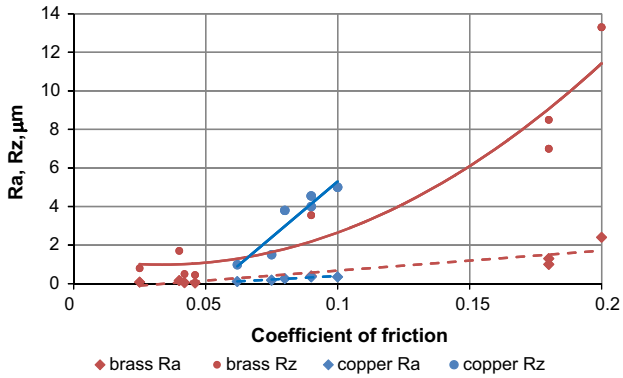

Fig. 5. The dependence between the friction coefficient and the roughness parameters, R_a and R_z for Cu and brass samples (the Gaussian filter is 0.8 mm).

the loads in the BL region for brass were significantly lower than for Cu samples (650–1050 N for brass in comparison to 1700–3200 N for Cu).

The morphology of rubbed surfaces after friction in the BL region is shown in Fig. 6. Friction of Cu samples is accompanied mainly with a delamination of thin films (Fig. 6a), while friction of brass samples is associated with a strong shearing of relatively thick sheets, Fig. 6b. These sheets present mainly α-phase, while in any depth the β-phase is appeared. A presence of the Pb on the surface of brass was revealed by EDS and considered bellow in the analysis of wear particles. Strong shearing is accompanied with severe plastic deformation of subsurface layers of brass up to the depth about 50 μm, Fig. 7a, whereas it is lesser than 10 μm for Cu.

High-magnified images of subsurface layers are shown in Fig. 8. Thin shear bands with the size of 1–3 μm are clear seen after

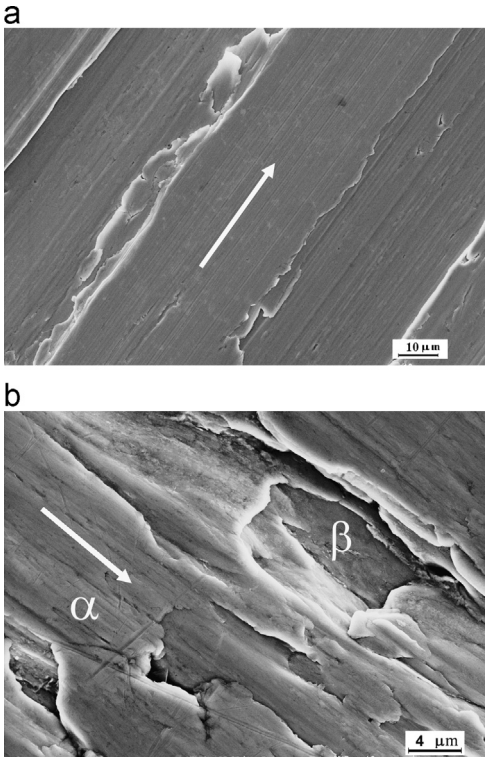

Fig. 6. SEM images of the surfaces of Cu, (a), $P=3100$ N, $\mu=0.09$ and brass, (b), $P=900$ N, $\mu=0.19$) after friction in the BL region. Sliding direction is shown by arrows.

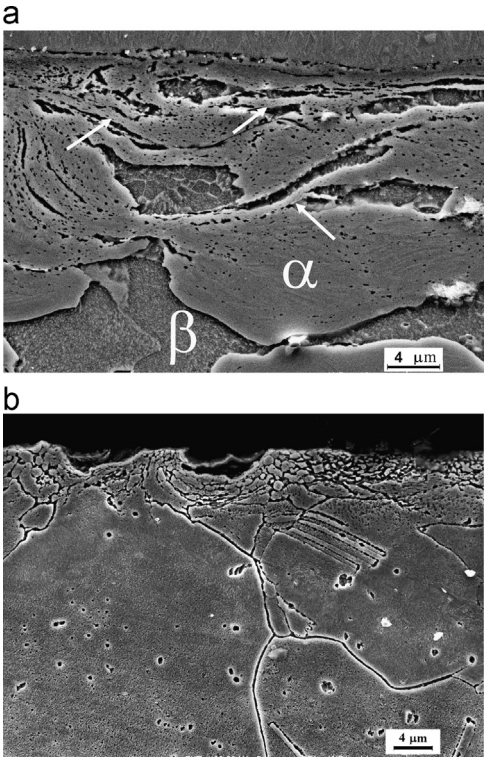

Fig. 8. Magnified images of cross-sectional ranges perpendicular to the wear track after friction in the BL region of brass (a) ($P=900$ N, $\mu=0.19$) and Cu (b) ($P=1750$ N, $\mu=0.08$).

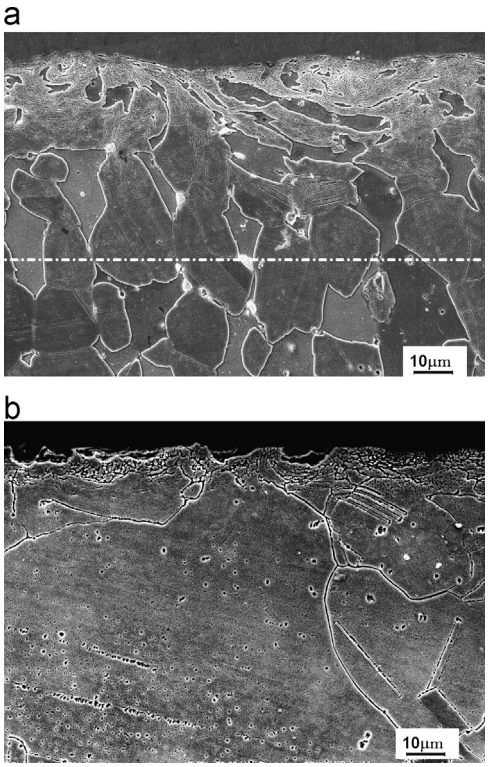

Fig. 7. SEM image of cross-sectional ranges perpendicular to the wear track of brass (a) ($P=900$ N, $\mu=0.19$) and Cu (b) ($P=1750$ N, $\mu=0.08$) after friction in BL region. White spots in the brass are Pb inclusions. A region of plastic deformation in brass is noted in (a).

deformation of α-phase grains, Fig. 8a, (showed by arrows), while small grains localized in the range of 3–4 μm are observed for Cu, Fig. 8b. Strong grain shearing in α-phase is accompanied with an

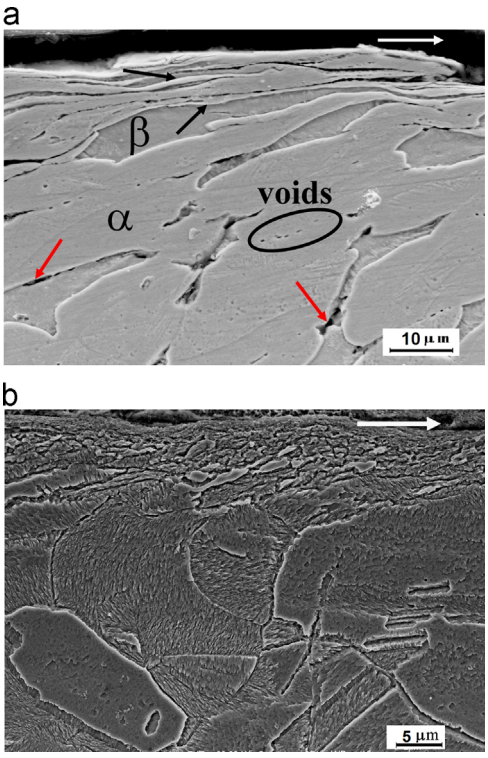

Fig. 9. SEM images of cross-sectional ranges in the direction of friction for brass (a) ($P=650$ N, $\mu=0.18$) and Cu (b) ($P=1750$ N, $\mu=0.08$). Shear bands are noted by black arrows. The cracks in the boundaries of α- and β-phases are depicted by red arrows (on the bottom of (a)). Some voids formed during a shearing are also noted in (a). (For interpretation of the references to color in this figure legend, the reader is referred to the web version of this article.)

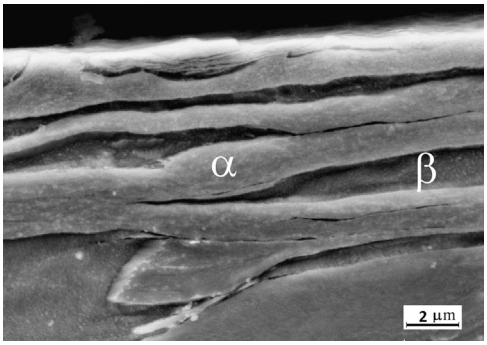

Fig. 10. SEM image of shear bands after friction of brass in the BL region.

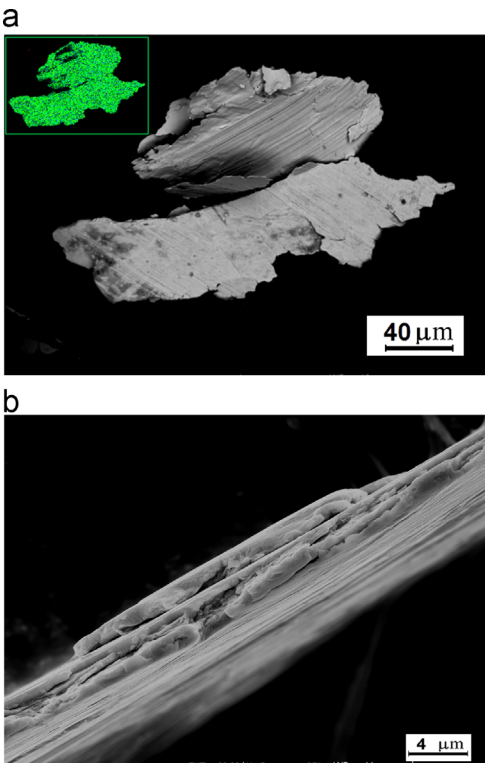

Fig. 11. SEM image of the wear particles of brass (α-phase) after friction in the BL region, (a); cross-sectional image of the wear particle, (b). In insertion, a distribution of Pb on the surface of wear particles.

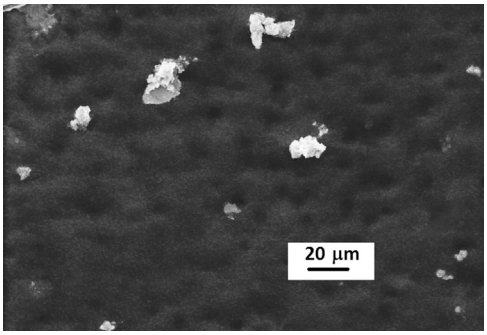

Fig. 12. SEM image of the wear particles of Cu after friction in the BL region.

enlargement of pores and microcracks in the boundaries or inside of the grains. A depth of the range of SPD and pore formation is about 20 μm. Cross-sectional images of subsurface layers cutting in the sliding direction are shown in Fig. 9. Strong shearing of α-phase grains is observed after friction of brass in the BL region,

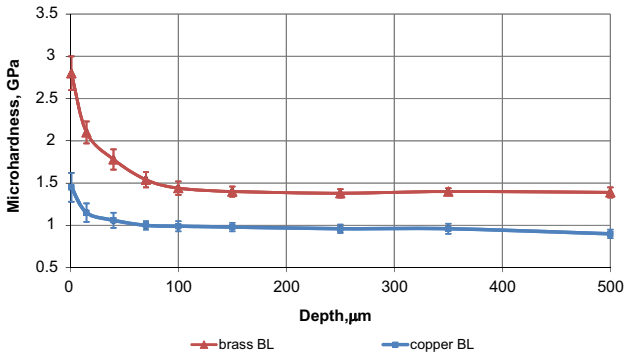

Fig. 13. A variation of the microhardness of subsurface layers upon a depth of the Cu and brass samples rubbed in the BL region.

Fig. 9a, while nanocrystalline structure is formed at thin surface layers of Cu, Fig. 9b. It can be seen that the size of virgin α-grains (~30 μm) decreased to the size about 1 μm due to strong shearing in thin surface layers, Fig. 9a. The deformation of β-phase is limited. Just some cracks are appeared in the boundaries of α- and β-phases, noted by red arrows in Fig. 9a. Intragranular fracture in α-phase associated with a coalescence of voids and cracks occurs during shearing in surface layers of α-phase. Thin layers of sheared α-phase grains can be considered as shear bands, noted by black arrows in Fig. 9a. Magnified image of shear bands after friction of brass in the BL region is shown in Fig. 10. The direction of shear bands is close to sliding direction of friction. A width of shear bands is 1–3 μm and this width corresponds to the size of wear particles. SEM image of the wear particles of brass after friction in the BL region is shown in Fig. 11.

The wear particles of brass in the BL region and a distribution of Pb on the surface of wear particles are shown in Fig. 11. The size of wear particles was varied from 10 μm to 250 μm. X-ray map in insertion demonstrates a presence of the Pb uniformly distributed on the surface of wear particles. The Pb, inclusions were also found in the grain boundaries and cracks, Fig. 8a, Fig. 9a and Fig. 10. The thickness of wear particles was close to the width of shear bands, see Fig. 10. It is interesting to note that the wear particles consists thin micro-scale sheets (Fig. 11b). In comparison to large and thick wear particles of brass, small particles with the size of some microns appeared in friction of Cu, Fig. 12.

In order to understand better the behavior of Cu and brass, a variation of the hardness vs. a depth was evaluated after friction in the BL region, Fig. 13. The hardness (strength) of thin surface layers for brass is significantly higher than for Cu samples (2750 MPa, and 1450 MPa, respectively). Deformation hardening (a difference between the hardness of deformed and virgin samples) for brass is 1400 MPa, while it is about 500 MPa for Cu samples.

4. Discussion

The present experiments revealed strong difference between the friction and wear behavior of Cu and brass. The friction coefficient, wear rate and depth of grooves are significantly larger for brass in the BL region, while the critical load of transition from the EHL to BL region is significantly lower in comparison to Cu. It is expected that this strong difference in the friction and wear behavior is associated with a different character of plastic deformation for Cu and brass. Severe plastic deformation of Cu rubbed in the BL region is localized in thin surface layers about some microns, while it is close to 20 μm for brass. Friction of Cu in the BL region is accompanied with formation of nanocrystalline structure with the grain size about 100 nm [23]. Friction of brass is attributed to superplastic deformation in thin surface layers of

α-phase grains due to compression and shearing. Intragranular slip as the accommodating mechanism occurs in α-phase, whereas little deformation is observed in β-phase. The accommodation of sliding during superplastic deformation accompanied with the growth and coalescence of pores, the formation and propagation of cracks, leading finely to delamination of wear particles. Our results indicate that intragranular slip in α-phase grains is the main mechanism of superplastic deformation under friction of brass in the BL region. As a result of superplastic deformation, shear bands practically parallel to direction of friction are formed during friction of brass in the BL region, Fig. 9a and Fig. 10. Two view-points were proposed in the analysis of superplasticity during tension of α/β brass at temperature about 600 °C [17–19]: the first one is the intragranular slip in β phase and the second one is the boundary sliding on the interface between α/β phases. It has been shown, as a confirmation of second view-point, that the main mechanism in tension of 59Cu40Zn1Pb brass at 600 °C is boundary sliding occurring on the α/β interphase [19]. Recently, it was shown that the temperature of superplasticity can be decreased up to 400 °C due to preliminary SPD of CuZn alloy [20]. Substantial grain refinement introduced due to preliminary ECAP processing and high angle α/β boundary sliding were proposed as dominant mechanisms of superplastic deformation. As it can be seen, superplasticity of α-phase grains in friction contradicts to the observed superplasticity of β-phase at high temperature in tension. It is known that β phase at the temperature lower than of 454 °C is hard and brittle [24]. In fact, the deformation of β-phase in friction was limited. Based on these results, it can be concluded that the flash temperature of brass–steel contact was lower than 454 °C. The measured temperature in the BL friction of brass was not more than 100 °C. We can just anticipate that superplastic deformation of brass is attributed to SPD of surface layers and a ductility of the α-phase at relatively high flash temperature of contact.

Main difference in the microstructural behavior of Cu and brass is the intragranular sliding in α-phase of brass accompanied with formation of shear bands, while nanocrystalline structure characterizes the friction process of Cu in the BL region. Our experiments agree well with the analysis of the microstructure of the low carbon 316 stainless steel in dry friction [25]. The structure and plastic deformation is explained by relatively low SFE in the low carbon 316 stainless steel. Shear bands in steel are formed also parallel to the direction of friction. The cracks are appeared mainly in the boundaries of shear bands. A similarity in the plastic deformation and the damage development during friction of F.C.C. α-phase of brass and stainless steel allows a suggesting that the SFE plays noticeable role in the plastic deformation, strain hardening and damage development of Cu and brass. Unfortunately, the effect of stacking faults in α-phase has not been studied till present time.

The Pb is a part of brass composition. Usually the Pb inclusions can play a dial role in friction and wear. From one side, the Pb is supplied to rubbed surfaces and thus can lead to decreasing the friction. From other side, the Pb inclusions presented in the cracks can accelerate their propagation. The Pb was found both on the rubbed surface and the surface of wear particles. However, although the Pb was revealed on rubbed surfaces, the friction coefficient remained high as usually observed in the BL region. Since the plastic deformation occurs in much thicker layers, the effect of Pb as lubricated material is limited at this case. The effect of the Pb inclusions on crack development will be especially considered in our future work.

Many voids and cracks are observed both in the boundary and inside of sheared grains of brass after friction in the BL region, Fig. 8a and Fig. 9a. The formation and distribution of voids can be probably initiated by intersection between primary and secondary slip systems due to the work hardening e.g. [26]. The formation and distribution of voids have been studied in more details in the analysis of material irradiation e.g. [27,28]. Unfortunately, the mechanism of void formation associated with the spatial distribution of defects during severe plastic deformation of F.C.C. materials remains unclear till the present time. It is naturally to anticipate that the shear bands formed during friction of brass initiate the voids, their coalescence, crack formation and their development. Possible mechanisms of the formation and distribution of voids in the friction of brass will be considered in our future work in more details.

Present experiments showed significantly higher deformation hardening and saturation hardness (stress) for brass in comparison to Cu. An increase of the deformation hardening with loading of brass during friction corresponds well with the analysis of the work hardening and saturation stress during plastic deformation of F.C.C. materials with low SFEs [12–16]. It is known that strain hardening of F.C.C. metals involve intersections of forest dislocations and cross slip. An increasing the saturation stress in low SFE's materials is explained by a difficulty of the cross slip and accordingly a slowing the recovery process even under relatively high temperature e.g. [29,30].

Let us now compare the mechanical properties of F.C.C. materials with high and low SFEs subjected to the SPD and friction in the BL region. It was shown the hardness and strength of Cu–Al, Cu–Zn and Cu–Ge alloys subjected to the SPD can be simultaneously enhanced through lowering the SFE [13–16]. However, the plastic deformation of these materials even in the early stages of subsequent deformation is accompanied with a plastic instability due to the formation of shear bands having a direct effect on failure initiation and crack development [31–33]. If plastic instability/shear bands during tension/compression lead usually to necking and finally to fracture, a superplastic deformation of brass is accompanied with formation of shear bands, voids and crack propagation and a shearing of the wear sheets. Principal difference between the fracture in the static, or dynamic (fatigue) and wear tests, is a continuation the plastic deformation after delamination of wear particles. A delamination and thus a creation of "fresh" surface can also stimulate the plastic deformation during friction. A steady state during superplastic deformation of surface layers is apparently supported by equilibrium between the processes of strain hardening and recovery. These aspects should be especially considered.

Finally, we would like to note that superplastic ductility of two-phase materials or ultrafine-grained materials at relatively high temperatures are especially attractive in metal forming process. However, the superplastic deformation in friction leads to formation thick and large wear particles and therefore to high wear rate. The materials as Cu with a localized deformation at thin surface ultra-fine grain layers can provide low friction and wear.

5. Conclusions

1. Friction, wear and plastic deformation of α/β brass and Cu rubbed in lubrication conditions were studied. The friction coefficient and wear of brass were significantly larger in comparison to Cu. The critical load of transition from the EHL to BL regions was two times lower for brass.
2. Friction of brass during the BL region is characterized by superplastic deformation of surface layers. Superplastic deformation of brass is attributed to intragranular sliding inside of α-phase grains and accompanied with a growth and coalescence of pores, formation and propagation of cracks, and development of wear particles. Strong shearing in surface layers of brass is accompanied with the formation of shear

bands. Thickness of wear particles is close to the width of shear bands.

3. Friction of Cu is attributed to localization of deformation at thin surface layers. Deformation hardening of surface layers of Cu in the BL region is significantly lesser than for brass.

References

[1] J.P. Hirth, D.A. Rigney, Crystal plasticity and the delamination theory of wear, Wear 39 (1976) 133–141.
[2] D.A. Rigney, W.A. Glaeser, The significance of near surface microstructure in the wear process (St. Louise, MO, April 25–28, 1977), in: W.A. Glaeser, K.C. Ludema, S.K. Rhee (Eds.), Proc. Int. Conf. on Wear of Materials, American Society of Mechanical Engineering, New York, NY, 1977, pp. 41–46.
[3] J.P. Hirth, D.A. Rigney, The application of dislocation conceptions in friction and wear, in: F.R.N. Nabarro (Ed.), Dislocations in Solids, North-Holland Publishing Co., Amsterdam, 1983, pp. 1–54 (Chapter 25).
[4] D.H. Backley, Possible Relation of Friction of Copper–aluminum Alloys with Decreasing Stacking-fault Energy (NASA TN D-3864), NASA Technical Note, Washington, 1967.
[5] P.J. Blau, A Study of the Interrelationship among Wear, Friction and Microstructure in the Unlubricated Sliding of Copper and Single Phase Binary Alloys (Ph.D. Dissertation), The Ohio State University, 1979.
[6] J.J. Wert, W.M. Cook, The influence of stacking fault energy and adhesion on the wear of copper and aluminium bronze, Wear 123 (1988) 171.
[7] F.A. Sadykov, N.P. Barykin, I.R. Aslanyan, Wear of copper and its alloys with submicrocrystalline structure, Wear 225–229 (1999) 649–655.
[8] M. Suery, B. Baudelet, Hydrodynamical behaviour of a two-phase superplastic alloy: α/β brass, Philos. Mag. A 41 (1980) 41–64.
[9] T. Küçükömeroğlu, L. Kara, The friction and wear properties of CuZn39Pb3 alloy under atmospheric and vacuum conditions, Wear 309 (2014) 21–28.
[10] A. Moshkovich, I. Lapsker, L. Rapoport, Correlation between strengthening and damage of Cu refined by different SPD processing and friction in different lubricant regions, Wear 305 (2013) 45–50.
[11] J.G. Sevillano, E. Aernoudt, P. van Houtte, Large Strain Work Hardening and Textures (Dislocations in metals), Elsevier Science & Technology Books (1981) 344.
[12] Q. Wei, Strain rate effects in the ultrafine grain and nanocrystalline regimes-influence on some constitutive responses, J. Mater. Sci. 42 (2007) 1709–1727.
[13] S. Qu, X.H. An, H.J. Yang, C.X. Huang, G. Yang, Q.S. Zang, Z.G. Wang, S.D. Wu, Z.F. Zhang, Microstructural evolution and mechanical properties of Cu–Al alloys subjected to equal channel angular pressing, Acta Mater. 57 (2009) 1586–1601.
[14] Z.J. Zhang, Q.Q. Duan, X.H. An, S.D. Wu, G. Yang, Z.F. Zhang, Microstructural and mechanical properties of Cu and Cu–Zn alloys produced by equal channel angular pressing, Mater. Sci. Eng., A 528 (2011) 4239–4267.
[15] J. Tao, K. Yang, H. Xiong, X. Wu, X. Zhu, C. Wen, The defect structures and mechanical properties of Cu and Cu–Al alloys processed by split Hopkins on pressure bar, Mater. Sci. Eng., A 580 (2013) 406–409.
[16] X.H. An, S.D. Wu, Z.F. Zhang, R.B. Figueiredo, N. Gao, T.G. Langdon, Enhanced strength–ductility synergy in nanostructured Cu and Cu–Al alloys processed by high-pressure torsion and subsequent annealing, Scr. Mater. 66 (2012) 227–230.
[17] J.W.D. Patterson, N. Ridley, Effect of phase proportions on deformation and cavitation of superplastic α/β brass, J. Mater. Sci. 16 (1981) 457–464.
[18] J. Belzunce, M. Suêry, Normalization of cavitation in superplastic α/β brasses with different phase proportions, Scr. Metall. 15 (1981) 895–898.
[19] H. Ding, Q. Wu, L. Ma, Deformation behavior in α/β two-phase superplastic brass, J. Mater. Sci. 27 (1992) 607–610.
[20] K. Neishi, Z. Horita, T.G. Langdon, Achieving superplasticity in a Cu-40% Zn alloy through severe plastic deformation, Scr. Mater. 45 (2001) 965–970.
[21] J.F. Archard, The temperature of rubbing surfaces, Wear 2 (1969) 438–455.
[22] Y. Wang, T. Lei, M Yan, C. Gao, Frictional temperature field and its relationship to the transition of wear mechanisms of steel 52100, J. Phys. D: Appl. Phys 25 (1992) A165–A169.
[23] L. Meshi, S. Samuha, S.R. Cohen, A. Laikhtman, A. Moshkovich, V. Perfilyev, I. Lapsker, L Rapoport, Dislocation structure and hardness of surface layers under friction of copper in different lubricant conditions, Acta Mater. 59 (2011) 342–348.
[24] J.R. Davis (Ed.), Copper and Copper Alloys, ASM International, 2001, p. 652.
[25] W.M. Rainforth, R. Stevens, J. Nutting, Deformation structures induced by sliding contact, Philos. Mag. A 66 (1992) 621–641.
[26] S.H. Tang, S. Wu, M. Kobayashi, H.L. Pan, Effect of texture evolution and point defects on ultrasonic waves under simple shear and pure shear, Int. J. Solids Struct. 44 (2007) 1277–1290.
[27] C.B. Carter, Observations on the climb of extended dislocations due to irradiation in the HVEM, Philos. Mag. A 42 (1980) 31–46.
[28] S.L. Dudarev, A.A. Semenov, C.H. Woo, Heterogeneous void swelling near grain boundaries in irradiated materials, Phys. Rev. B: Condens. Matter 67 (2003) 094103–094115.
[29] Y Zhang, N.R. Tao, K. Lu, Effect of stacking fault energy, strain rate and temperature on microstructure and strength of nanostructured Cu–Al alloys subjected to plastic deformation, Acta Mater. 59 (2011) 6048–6058.
[30] Y.L. Gong, C.E. Wen, X.X. Wu, S.Y. Ren, L.P. Cheng, X.K. Zhu, The influence of strain rate, deformation temperature and stacking fault energy on the mechanical properties of Cu alloys, Mater. Sci. Eng., A 583 (2013) 199–204.
[31] M.A. Meyers, Y.B. Xu, Q. Xue, M.T. Perez-Prado, T.R. McNelley, Microstructural evolution in adiabatic shear localization in stainless steel, Acta Mater. 51 (2003) 1307–1325.
[32] T.S. Byun, N. Hashimoto, K. Farrell, Temperature dependence of strain hardening and plastic instability behaviors in austenitic stainless steels, Acta Mater. 52 (2004) 3889–3899.
[33] E.A. El-Danaf, A. Al-Mutlaq, M.S. Soliman, Role of stacking fault energy on the deformation characteristics of copper alloys processed by plane strain compression, Mater. Sci. Eng., A 528 (2011) 7579–7588.